

Experimental Details

Materials. The PEDOT:PSS (Clevios PH 1000, 1 wt%) aqueous dispersion was purchased from Heraeus. Waterborne polyurethane (PU) was provided by DSM (China). Poly(dimethylsiloxane) (PDMS, Sylgard 184, Dow Corning) prepolymer was prepared by mixing base silicone gel with a curing agent in a 10:1 weight ratio. Dimethyl sulfoxide (DMSO) was purchased from Aladdin Chemistry Co., Ltd., Shanghai, China. Ethyl acetate and hydrochloric acid (HCl) were obtained from Shanghai Lingfeng Chemical Reagent Co., Ltd., Shanghai, China. All reactants were analytical purity and used as received. Deionized (DI) water was used throughout the experiments.

Fabrication of G/PEDOT:PSS/PDMS composite

The nickel (Ni) foam was cut into desired size followed by soaked in 1M HCl for 15 min, and washed with distilled water. After immersed in ethanol for 1 min and dried at 50 °C for 5 min (0.1 Mpa), the Ni foam was taken out rapidly and put into a horizontal furnace. The furnace was heated to 1000 °C within 100 min under a mixed air source of hydrogen (H₂, 200 s.c.c.m.) and argon (Ar, 500 s.c.c.m.), and kept for 5 min to remove a few layers of Ni oxide on Ni surface. Later, methane (CH₄) as a carbon source was introduced with a flow rate of 10 s.c.c.m., and the reaction time was controlled between 5 min to 20 min. Then the CH₄ was closed and the furnace was cooled to room temperature with the rate of 100 °C/min. Finally, the CVD graphene/Ni foam (GF) was obtained.

The waterborne PU was mixed with PEDOT:PSS aqueous solution (with 5 wt% DMSO), and their weight ration was set at 1:5. Then the GF sample was dipped into the prepared solution, and vibrated for 10 min. Afterwards, the sample was dried at 90 °C for 10 min and then taken out to cool to ambient temperature. The fabricated GF/PEDOT:PSS composite was immersed into a dilute PDMS organic solution (a mixture of PDMS base agent, curing agent and ethyl acetate in a ratio of 30:3:100) for 30 min, and followed by thermally curing at 100 °C for 1 h in vacuum. The Ni was etched by ferric nitrate (Fe(NO₃)₃) solution (1M). Finally, after dried by freeze-drying, the porous CVD graphene/PEDOT:PSS/PDMS (CGPP) was obtained.

In this article, porous CVD graphene/PDMS (CGP) was also prepared as a reference sample. The Ni foam/CVD graphene was directly immersed into the dilute PDMS organic solution for 30 min and cured at 100 °C for 1 h in vacuum. After removing Ni by 1M Fe(NO₃)₃ solution, the CGP was successfully prepared.

Characterization.

The morphologies of the CGP and CGPP were examined by using a field emission scanning electron microscopy (FE-SEM, Hitachi S-4800), operating at 5kV. The morphology and small angle x-ray scattering (SAXS) of CVD graphene were characterized by transmission electron microscopy (TEM). Raman spectra of the CVD graphene was collected on a Lab Ram Infinity Raman spectrometer, using a linearly 514.5nm lasers. The water contact angles of the mixture solutions of PU and PEDOT:PSS with different ratios were detected by a contact angle measurement instrument (JC2000D3) on a Ni foil with graphene coating. The electrical conductivity of CGP, CGPP (with and without PU) composite films were measured by four-point probes (model RTS-8, Guangzhou 4Probes Tech Industrial Co., Ltd., Guangzhou, China) contact direct current (dc) conductivity measurement method at room temperature. The tensile tests were performed using a universal testing machine (CMT 4204, Sansi Co., Ltd., China).

Supporting results

Fig. S1 shows the TEM image, SAXS as well as Raman spectra of GF, respectively. As can be seen from high-resolution TEM (Fig. S1a), the CVD graphene on Ni foam illustrates mono-, tri- and four-layers sheets clearly, which is consistent with the results from Raman spectra (the ratio of I_G/I_{2D} peaks is in the range of 0.69 to 1.22, indicating the range of CVD graphene layers is mono- to few-layers). Besides, the interlayer spacing of graphene sheets is ~ 0.34 nm, which is very close to the theoretical value of 0.335 nm. SAXS shows triple spots of 6-fold symmetry, elucidating three layers structure of graphene (Fig. S1b). Meanwhile, in the Raman spectra, the structural defects related D peak can hardly be observed, which means that the CVD graphene features high quality and structural integrity.

The GF was dipped into a dilute PEDOT:PSS (~ 0.1 wt%) aqueous solution and dried in oven at 90°C in vacuum, as shown in Fig. S2a, we can clearly see that the porous scaffold was coated by PEDOT:PSS completely. However, as shown in the magnified SEM images (Fig. S2b and c), some crevices appeared on PEDOT:PSS coating, which is detrimental to both the electrical and mechanical properties of GF/PEDOT:PSS skeleton. Even if the concentration of PEDOT:PSS was increased by a factor of ten (~ 1 wt%, Fig. S2d), the cracks were still existed (Fig. S2e and f). These phenomena are presumably because the evaporation rate (ER) of water in different regions of the 3D scaffold at 90°C is diversely. The region with higher ER generates solid particles first, which would impact the fluxion of solution and cause film defects.

To overcome the cracks problem in PEDOT:PSS coating during solvent evaporation process, the water was replaced by high boiling point solvent ethylene glycol (EG), because the ER of EG is comparatively uniformly throughout the whole GF scaffold at 90°C . The morphologies of the obtained GF/PEDOT:PSS composite are shown in Fig. S3. It can be clearly seen from Fig. S3b that no fractures present on the PEDOT:PSS coating, which demonstrates that the evenly distributed ER of solvent in porous framework is very useful for eliminating cracks. However, it is also found that the thickness of PEDOT:PSS coating on the GF scaffold is non-uniformly, moreover, in the inner parts of the porous structure (Fig. S3c), the scattered PEDOT:PSS cannot form a connected film on CVD graphene. Therefore, with a solvent of either a high boiling point EG or water, the obtained PEDOT:PSS coating both showed a defective and discontinued conductive network. To overcome these problems, we developed a new strategy by using the mixed solution of waterborne PU and PEDOT:PSS aqueous solution to coat the GF scaffold, and the result demonstrates that an integrity and connected PEDOT:PSS coating was formed on the porous GF structure (Fig. 1d and e).

The waterborne PU would increase the wettability between the PEDOT:PSS aqueous solution and graphene sheets, contact angle (CA) measurement was used to assess this property. Graphene oxide ethanol solution was primarily covered on Ni film, and the graphene/Ni was obtained after drying and reduction processes, which is served as the substrate. The PEDOT:PSS and waterborne PU was mixed by different mass ratio, and these mixtures were separately used for dipping of the graphene/Ni substrate. It can be seen from Fig. S4 that the CA of pure PU aqueous solution on graphene was $\sim 80^\circ$ as a result of high viscosity of pure PU. When the PEDOT:PSS was introduced into the pure PU aqueous solution with a mass ratio of 1:1, the CA significantly dropped to 67° , indicating that the wettability of solution is improved. Then, further increasing the content of PEDOT:PSS and made a mass ratio of 5:1, a minimum CA ($\sim 55^\circ$) was obtained. Interestingly, the CA between the mixed solution and graphene increased again with enhanced

content of PEDOT:PSS. When their mass ratio increased to 10:1 and 20:1, the CA reached a stable value of $\sim 65^\circ$. Thus, we chose the mixed solution of PEDOT:PSS and PU with a mass ratio of 5:1 to coat the GF framework structure.

When the mixed solution of PEDOT:PSS and PU with a mass ratio of 5:1 was used, the boiling point of the solution raised and the CA of it on graphene declined markedly, resulting in a significantly improved wettability. Thus, the PEDOT:PSS would coat on 3D GF skeleton uniformly and completely. As shown in Fig. S5, graphene sheets on both the outer and internal framework of GF were covered by PEDOT:PSS thin layers with smooth and integrity surfaces. The PEDOT chain formed a mesh structure, and the voids in the network were filled with PU molecules. The PU enhanced the connection between PEDOT:PSS thin layer and graphene after drying. Therefore, a certain amount of waterborne PU can solve the above-mentioned problems of film broken and uneven coating.

The conductivity of CGPP as a function of the mass ratio between PEDOT:PSS and CVD graphene was investigated by keeping the overall mass ratio of the conductive fillers at 7.5 wt%. As shown in Fig. S6, when the mass ratio of graphene and PEDOT:PSS was 1:3, the composite possessed a conductivity of 45 S cm^{-1} . At this point, the content of PEDOT:PSS far exceeded that of graphene resulting in excessive overlying PEDOT:PSS on graphene surface. Therefore, the composite tended to show the electrical conductivity of PEDOT:PSS, which restricted the synergistic effect between the two components. As the content of PEDOT:PSS reduced, the doping effect of conducting polymer to graphene became more apparent. At the mass ratio of 1:2, the conductivity of CGPP composite reached 65 S cm^{-1} . When the two constituents showed the equal mass, the doping effect of PEDOT:PSS to CVD graphene got more obvious. It is presumably that both the quality and thickness of PEDOT:PSS layer deposited on graphene are more suitable for attracting and transferring electrons, so that electrons could transfer between graphene sheets more easily. Hence, a highest conductivity of 73 S cm^{-1} was reached in this situation. However, further reducing the amount of PEDOT:PSS would weaken the doping effect because only a certain degree of hindrance between graphene sheets was eliminated, which resulted in a lower conductivity of 47 S cm^{-1} in a mass ratio of 2:1. As a consequence, the mass ratio of PEDOT:PSS and CVD graphene controlled at 1:1 was chosen to prepare CGPP composite.

We also coated a layer of PEDOT:PSS and PEDOT:PSS/PU hybrid on PDMS film, respectively. The conductivities of PEDOT:PSS/PU/PDMS and PEDOT:PSS/PDMS composites as a function of tensile strain is shown in Fig. S7. It can be seen that PEDOT:PSS/PU/PDMS film exhibits slower increment of resistance, which is attributed to the positive action of stretchable PU (the PU resin we chose possesses a certain stretchability of $\sim 100\%$). Hence, with the aid of PU, the PEDOT:PSS/PU/PDMS film could adopt the integral deformations, resulting in relatively slower change of resistance during the stretching process, which also demonstrated more excellent performance of CGPP compared to CGP.

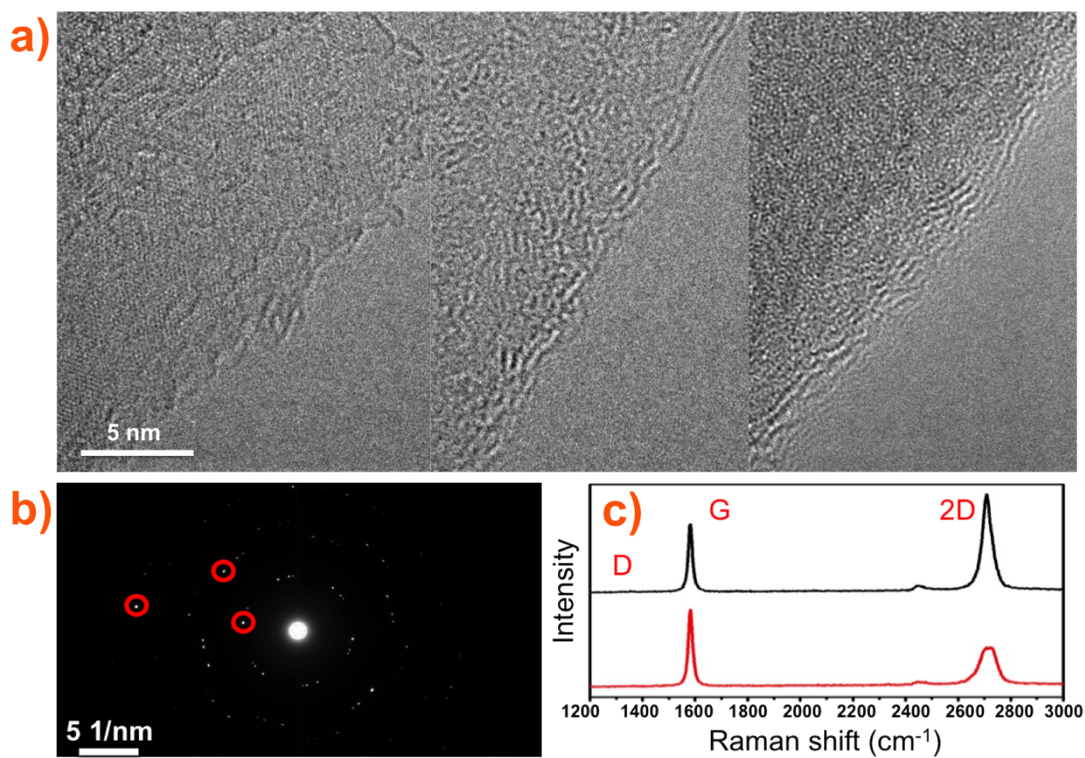


Fig. S1 (a) High-resolution TEM images of graphene sheets with different numbers of layers in a GF. (b) The SAXS of GF. (c) Typical Raman spectra of a GF.

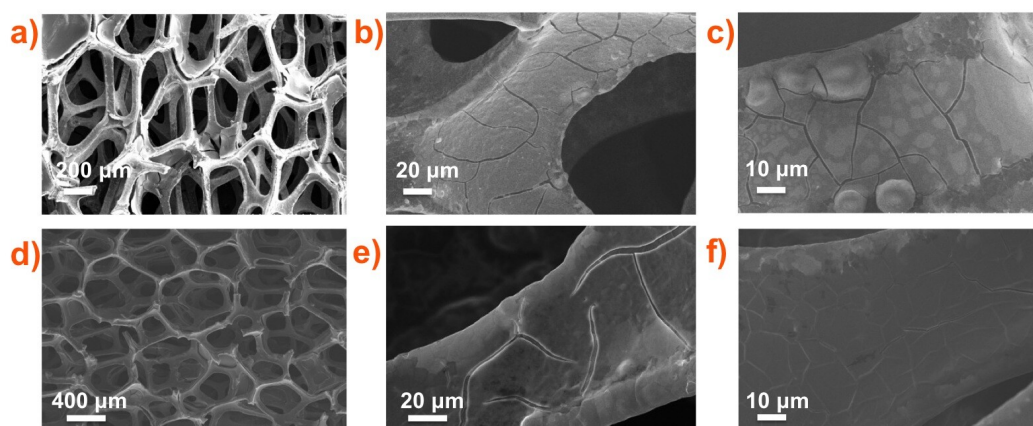


Fig. S2 SEM images of GF coated with (a) (b) (c) dilute PEDOT:PSS aqueous solution (~0.1 wt%) and (d) (e) (f) concentrated PEDOT:PSS aqueous solution (~1 wt%).

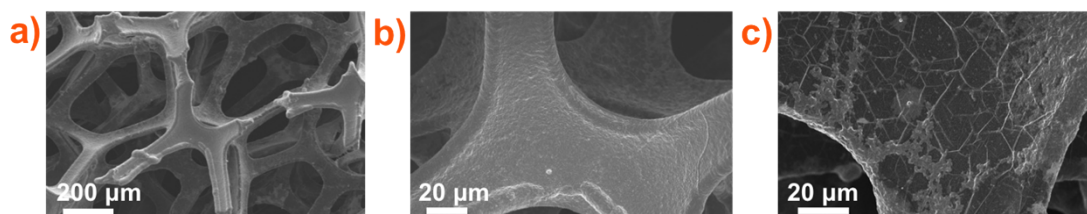


Fig. S3 SEM images of GF coated with PEDOT:PSS ethylene glycol solution.

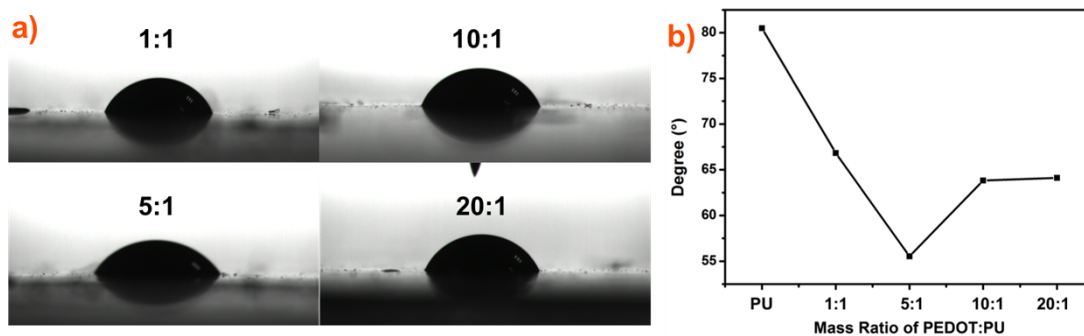


Fig. S4 The contact angles of PEDOT:PSS/PU mixed solution to graphene film as a function of mass ratio of PEDOT:PSS to PU.

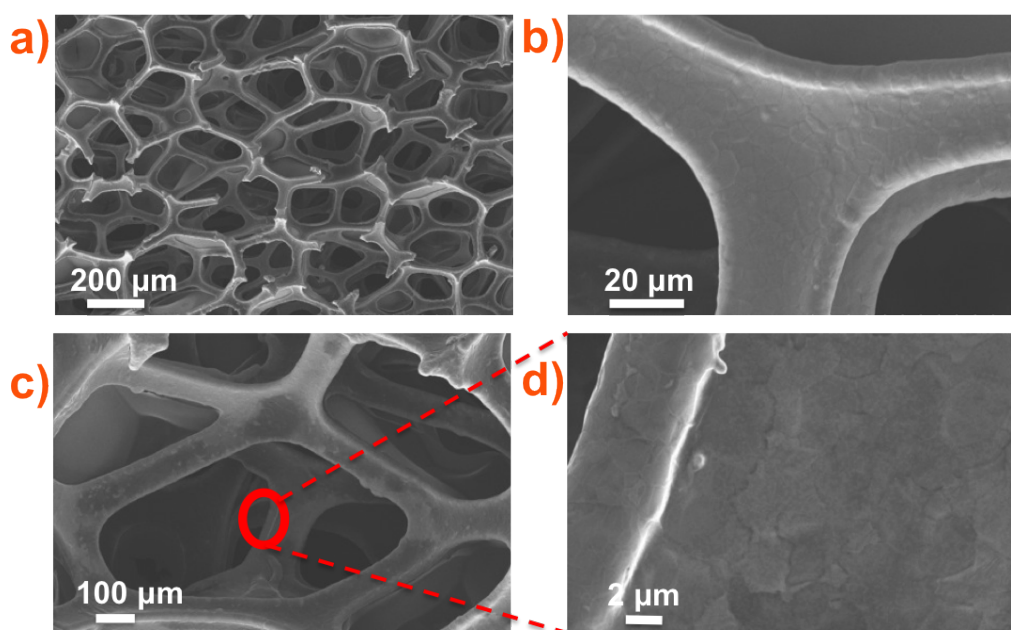


Fig. S5 SEM images of GF coated with PEDOT:PSS/PU mixed solution by a mass ratio of 5:1.

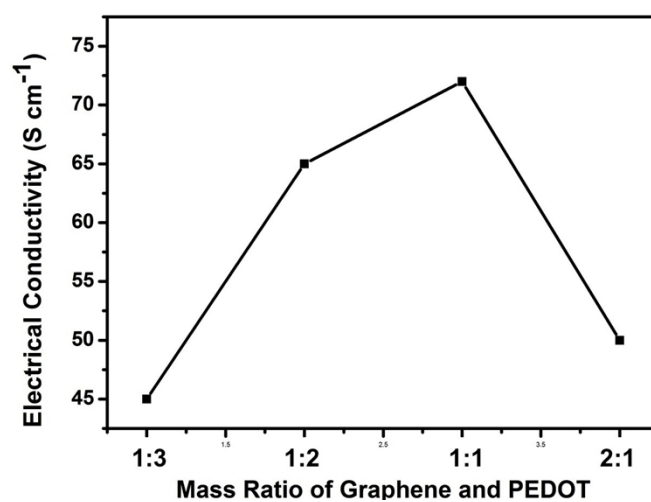


Fig. S6 The conductivity of CGPP as a function of the mass ratio of graphene and PEDOT.

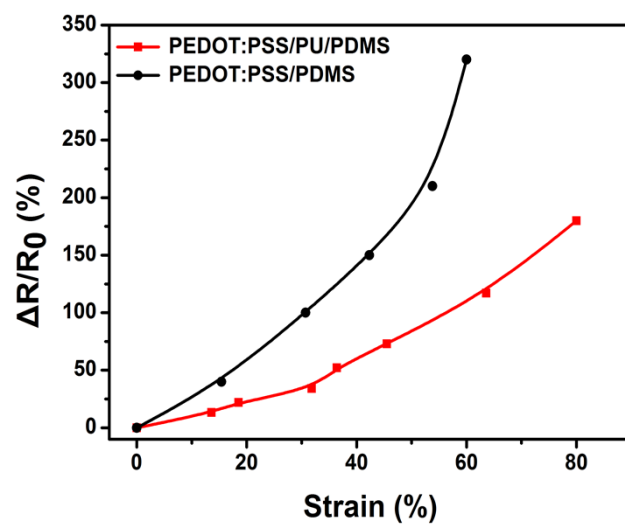


Fig. S7 Electrical-resistance variation of PEDOT:PSS/PDMS and PEDOT:PSS/PU/PDMS films as a function of tensile strain.